

Magnetite Particle Size Dependence on the Co-precipitation Synthesis Method for Protein Separation

Raúl Terrazas Reza, Carlos A Martínez Pérez, A Martínez Martínez and Perla E García-Casillas*

Instituto de Ingeniería y Tecnología, Universidad Autónoma de Ciudad Juárez, Ave. Del Charro #610 norte, C.P. 32320, Cd. Juárez Chihuahua, México.

* pegarcia@uacj.mx or perlaelviagarcia@yahoo.com

ABSTRACT

In this work, the synthesis of magnetite nanoparticles by a three variant chemical co-precipitation methods that involves reflux and aging conditions as well as slow and rapid injection techniques was investigated. The synthesized magnetite nanoparticles showed a spherical shape with an average particle size directly influenced by the synthesis technique. Average particle size from 16 nm, 27 nm and 200 nm were obtained. All three types of magnetite nanoparticles had a superparamagnetic behavior and their saturation magnetization is influenced by the particle size. Values of 56, 67 and 78 emu/g were obtained for the 16 nm, 27 nm and 200 nm magnetite particles, respectively. The protein adsorption was improved by using a surface coating. The silica-aminosilane coating showed the best performance followed by the aminosilane coating. The silica coating showed the lowest adsorption for all three particle sizes.

Keywords: Nanoparticles, magnetite, chemical co-precipitation, protein separation, polymer coating

1 INTRODUCTION

The size of magnetic particles plays a key role for their applications and nanoparticles have shown extraordinary results compared to micro and macro scale particles [1-2]. In the nanometric scale, each particle contains a simple magnetic domain and shows a superparamagnetic behavior, which gives a rapid response to magnetization and demagnetization when an external magnetic field is applied and removed, respectively [2-4]. This kind of magnetic response is desired in applications where high precision is required to direct them easily and quickly. It offers the possibility of manipulating the magnetic nanoparticles by applying a magnetic field which makes them very attractive [5-7]. Many of these types of nanoparticles are metallic, which are not stable and are easily oxidized, therefore their applications are limited. Metallic oxides nanoparticles can overcome this limitation. Magnetite (Fe_3O_4) has been widely used in the field of magnetic materials [8-9]. In recent years, considerable effort has been focused in the

design and controlled synthesis of this material with certain shape and particle size. These properties are crucial in the performance of the magnetic nanoparticles [10-12]

The synthesis of magnetic particles with the desired shape, size, and uniform size distribution, is a very important step that needs to be first achieved before any further research and use. A uniform particle size distribution is highly desired because magnetic properties show a strong dependence on the nanometric scale [10-16].

Based on the fact that different synthesis methods leads to particles with different size and morphology, this research is focus on the influence of the co-precipitation methods for the synthesis of magnetite particles and the processing parameters. Fast versus slow nucleation rates and nucleation with refluxing and aging conditions were evaluated. In order to use the magnetic nanoparticles for protein separation, they were coated with different types of materials obtaining specific superficial properties and making them suitable for attaching biological materials to their surface [17-22]. Different superficial functional groups were used: aldehyde (-CHO), hydroxyl (-OH) and amine (-NH₂).

2 EXPERIMENTAL PROCEDURE

The magnetite nanoparticles were coated with silica by dissolving 0.1910g of sodium metasilicate in 10 ml of water and adding 0.020 g of nanoparticles. The mixture was ultrasonically agitated during 30 min, and heated up to 80°C. The pH of the solution was lowered to 6 using HCl and a composite was obtained. The obtaining powder was centrifuged and washed several times until a pH of 7 in order to remove the residual ions; the powder was dried at 35°C during 24 h.

The coating of the aminosilane shell was obtained by mixing 100 μL of N-(2-aminoethyl)-3aminopropyltrimetoxysilane (AEAPS), 0.02 g of magnetic nanoparticles and 25 μL of deionized water in 2.5 mL of methanol. The mixture was exposed to ultrasonic agitation for 30 minutes and then 1.5 mL of glycerol was added. The solution was heated up to 85°-90°C, and a high mechanical agitation was kept during 6 h. The obtained precipitate was washed with water and methanol 4 times in each case. 15 mL of glutaraldehyde were added and the mixture was

agitated ultrasonically for 45 min. Finally, the precipitate was washed with water and dried at 20°-35°C for 24 h. A combined coating of silica and aminosilane was also applied. The nanoparticles were coated in two steps: silica coating was applied first followed by the aminosilane shell using the methodologies already described.

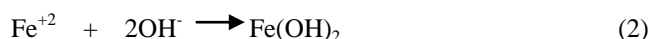
The protein immobilization over magnetite was evaluated using four different surface conditions: pure magnetite –no coating- (M sample), magnetite with silica coating (M-S sample), magnetite with aminosilane coating (M-A sample) and magnetite with silica and aminosilane coatings (M-S-A sample). Bovine Serum Albumin (BSA) was used as standard protein. A BSA solution with a concentration of 2 µg/µL was prepared. During each protein adsorption assay, a calibration curve was run using BSA concentrations going from 0 to 2.0 µg/µL, with increments of 0.2 µg/µL. The protein immobilization was achieved by mixing 10 µg of nanoparticles with different initial concentrations of BSA in a total volume of 300 µL, going from 0 to 1.33 µg/µL. The incubating conditions were under room temperature, with vigorous continuous agitation (Vortex®) and for a period of time of 30 min. Protein adsorption was determined using the Bradford colorimetric method at 595 nm visible light wavelength.

X-Ray Diffraction (XRD) was used to confirm the magnetite (Fe₃O₄) phase in each synthesis method. The size distribution and morphology of nanoparticles were characterized by Field Emission Scanning Electron Microscope (FE-SEM), and the elemental chemical analysis was performed by Energy Dispersive X-ray Spectroscopy (EDS). The magnetic properties were obtained using a Vibrating Sample Magnetometer (VSM). Protein adsorption on magnetite nanoparticles was studied by determining the amount adsorbed using a Visible Light Spectrometer.

3 RESULTS AND DISCUSSION

3.1 Suggested mechanism of magnetite nanoparticles formation

The following chemical reaction mechanism occurred in the three methods: trivalent iron ion hydrolyzes forming (FeOOH) (eq. 1) as pH increases; divalent iron ion forms Fe(OH)₂ (eq. 2) under alkaline conditions. Both chemical species reacted with each other at pH values of around 10 to 11, forming magnetite according to Cornell et al. equation (eq. 3). The overall chemical reaction is represented by equation 4:



The formation of all the intermediate species were not characterized, but the use of divalent and trivalent iron precursors (Fe⁺³ and Fe⁺²) and the pH conditions kept during reaction support the suggested mechanism based on discussed theory [1].

The chemical co-precipitation method with slow injection differs from the rapid injection method on the addition rate of ammonium hydroxide, which has a direct effect in how fast the pH change to favor the magnetite formation. In the chemical co-precipitation method with reflux and aging, the desired pH condition was obtained through the decomposition of urea at high temperature, and is represented by the following chemicals reactions [14,15].



3.2 Chemical, morphological characterization and properties.

The XRD pattern of the three synthesized nanoparticles is shown in figure 1. According to these results, it is observed that all three sample spectra are similar among them, and they are similar to the pure magnetite XRD spectrum. Pure magnetite shows six characteristics diffraction peaks, which were obtained in the three methodologies. Miller index notation is used. An inverse spinel crystal structure was obtained.

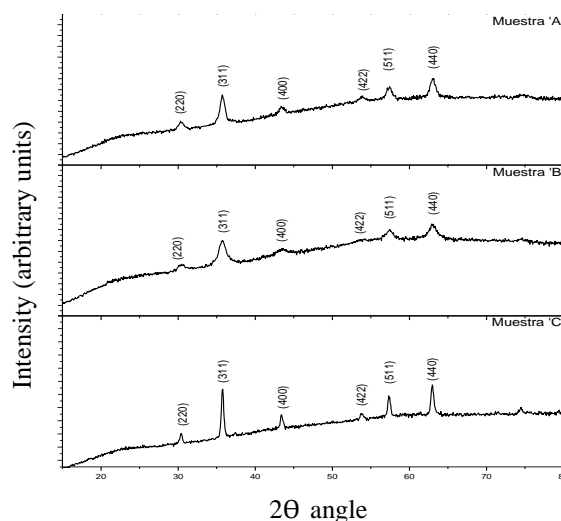


Figure 1: XRD spectra of (C) co-precipitation with reflux and aging method, (B) chemical co-precipitation with slow and (A) fast injection methods.

The obtained XRD patterns showed differences in the peak width, which is due to the different crystallite size. Wide peaks indicate the small crystals presence while narrow ones indicate larger crystals. Magnetite made with a slow and reflux method showed similarity in peaks width; however sample made with fast injection method showed smaller values. The average values of the Full Width at Half Maximum (FWHM) for the three samples is shown in table 2. It can be observed that the sample obtained by co-precipitation with reflux and aging method showed bigger crystal size than those observed in samples obtained by chemical co-precipitation with slow and fast injection methods, which showed similar values between them.

Table 2. FWHM values for the three magnetite samples.

Position 2 θ	FWHM (2 θ)		
	Co-precipitation with reflux and aging variant	Co-precipitation with slow injection variant	Co-precipitation with fast injection variant
30.362	0.6888	0.7872	0.2460
35.765	0.3936	0.3936	0.2460
43.473	0.7872	0.6888	0.1968
53.946	0.7872	0.9840	0.3936
57.512	0.6888	0.7872	0.2952
63.166	0.7200	0.8400	0.4200

The morphology of the Magnetite nanoparticles was observed by FE-SEM. All three samples exhibit spherical particle shape. The difference observed among samples was regarding the particle size. Magnetite obtained by co-precipitation with reflux and aging method showed higher particle size than magnetite obtained by chemical co-precipitation with slow and fast injection methods, the last one showed the smallest size.

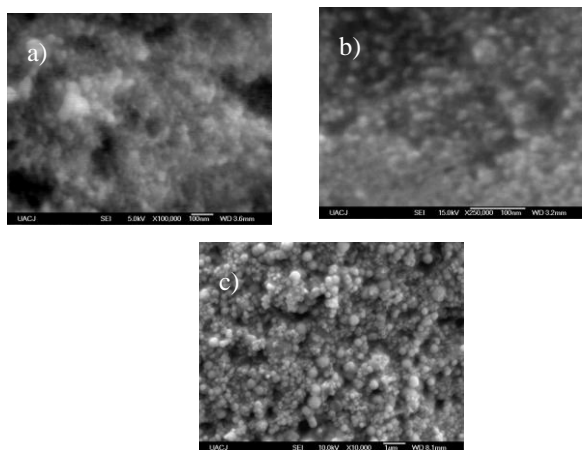


Figure 2: FESEM micrograph of magnetite obtained by a) co-precipitation with slow and b) fast injection methods, and c) co-precipitation with reflux and aging method

The figure 3 shows the average particle size and size distribution for each one of the samples. According to these results, magnetite obtained by fast injection method showed the smallest average particle size and more uniformity on particle size distribution than magnetite obtained by slow injection and with reflux and aging method, as it is established by the standard deviation values.

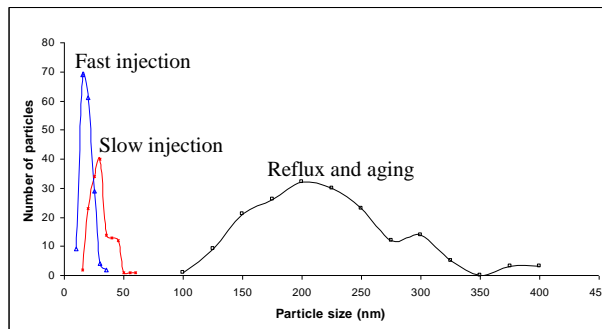


Figure 3: Particle size distribution

Magnetite obtained by reflux and aging showed the highest saturation magnetization of 78.21 emu/g and the magnetite obtained by rapid injection exhibits the smallest value (55.98 emu/g); magnetite obtained by slow injection showed a value of 64.33 emu/g. The hysteresis loop shows that all three samples present a superparamagnetic behavior, which is suitable for protein separation in biomedical applications. As result of the different method used, three different nanoparticles sizes werer obtained. Figure 4 shows the behavior of the saturation magnetization (M_s) as function of particle size and coatings. In all cases, the coating dismishit the M_s . However the aminosilane coating has a lower effect than silica.

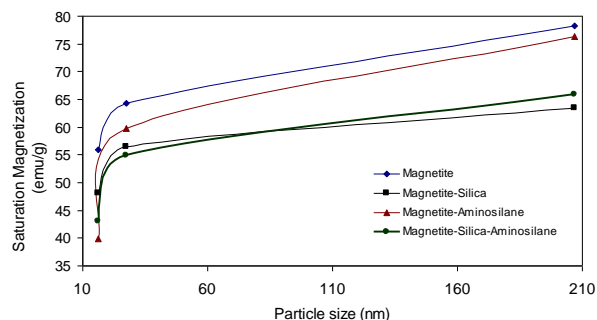


Figure 4: Saturation magnetization dependence over magnetite particle size

The coating of the particles was confirmed by FTIR analysis (figure 5). No significant differences were found between the three types of magnetite particles. The magnetite particles (M) show the characteristic band of Fe-O bond at 590 approximately but when these particles are coated with silica a new band appears at 1072 cm^{-1} due to Si-O bond (M-S) [19]; this band is present when the

particles were coated with silica (M-S) and silica-aminosilane (M-S-A). In the FTIR spectra of M-A and M-S-A samples, bands at 3309 and at 1654 cm^{-1} were observed, which are attributed to the amine group ($-\text{NH}_2$) [12]. The band at 2943 cm^{-1} is due to the stretching of C-H of the methyl group ($-\text{CH}_2$, $-\text{CH}_3$). When the particles have a silica shell (Silica-Aminosilane Coating-MAS sample), a new band is shown at 802 cm^{-1} due to Si-O-Si bond [23].

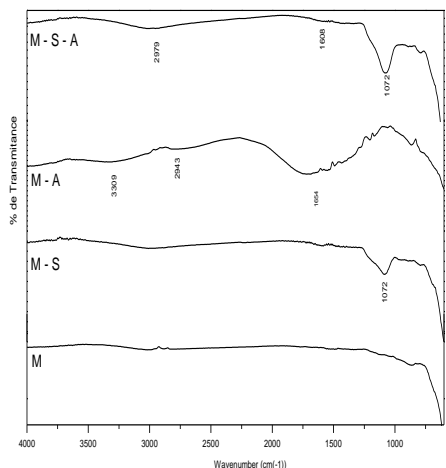


Figure 5: FTIR of magnetite (M), magnetite with silica coating (M-S), magnetite with aminosilane (M-A) and magnetite with silica and aminosilane coating (M-S-A)

The amount of Albumin Serum Bovine (BSA) protein used to immobilize the nanoparticles surface is influenced by the type of coating present, and in all cases it is superior to that observed on pure magnetite. Magnetite-aminosilane (MA) and Magnetite-silica-aminosilane (MSA), had higher capability for protein adherence than silica coating and pure magnetite (no coating). MSA showed a maximum protein retention capacity for all three magnetite particle sizes. Figure 6 shows the relationship between protein adsorption, surface coating and particle size. The best combination (regarding functionality) for the higher protein adsorption is small magnetite particles (16nm) with silica-aminosilane coating.

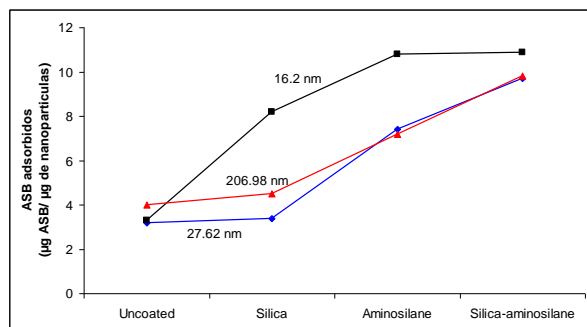


Figure 6: Protein adsorption capacity as function of particle size and coating type.

4 CONCLUSION

- The nucleation rate and growth speed during magnetite synthesis have a direct influence on the particle size. Under reflux and aging conditions, the formation of large particles (200 nm) is favored but under rapid injection conditions, small particles were obtained (16 nm). More uniformity in particle size was observed when small particles were obtained. The standard deviation values of the average particle size were 4 nm for 16 nm particle size, 8 nm for 27nm and 59 nm for the largest particles (200 nm).
- The magnetite nanoparticles coatings improved their protein adsorption capability with no detriment on their superparamagnetic behavior.
- The type of functional group present on the coating influences the protein adsorption. The silica-aminosilane coating showed the highest protein adsorption capacity in all magnetite nanoparticles studied.
- The best combination to obtain the highest protein adsorption is when an average particle size of 16nm coated with silica-aminosilane coating is used.

REFERENCES

- [1]. Cornell, R.M., Schwertmann, U. 2003. The iron oxides: Structure, Properties, Reactions, Occurrences and Uses. Segunda edición. Wiley-VCH GmbH & Co. Egaa.
- [2]. Cao, Guozhong. 2004. Nanostructures & nanomaterials: Synthesis, Properties & Applications. Imperial Collage Press.
- [3]. Cullity, B. D., 1971. Introduction to Magnetic Materials. Addison-Wesley Publishing Company, Inc.
- [4]. Jiles, 1991. Introduction to Magnetism and Magnetic Materials. Ed. Chapman & Hall. 1era edición. Londres, Inglaterra.
- [5]. Rossi, L., Quach, A., Rosenzweig, Z., 2004. Glucose oxidase-magnetite nanoparticles bioconjugate for glucose sensing. Springer-Verlag. Anal Bioanal Chem 380: 606-613. DOI 10.1007/s00216-004-2770-3.
- [6]. Schmid, G. 2004. Nanoparticles: From Theory to Application. Wiley-VCH Verlag GmbH / Co. KGaA.
- [7]. Wang, J., Peng, Z., Huang, Y., Chen, Q. 2004. Growth of magnetite nanorods along its easy-magnetization axis of [1 1 0]. Elsevier Journal of Crystal Growth 263 616-619.
- [8]. Schüth, F., Lu, A., Salabas, E.L., 2007. Magnetic Nanoparticles: Synthesis, Protection, Functionalization, and Application. Angewandte Chemie, Wiley-VCH Verlag GmbH & Co. KGaA, Weinheim. DOI: 10.1002/anie.200602866

- [9]. Osaka, T., Matsunaga, T., Nakanishi, T., Arakaki, A., Niwa, D., Iida, H., 2006. Synthesis of magnetic nanoparticles and their application to bioassays. Springer-Verlag. Anal Bioanal Chem 384: 593-600. DOI 10.1007/s00216-005-0255.7.
- [10]. Gnanaprakash, G., Mahadevan, S., Jayakumar, T., Kalyanasundaram, P., Philip, John., RAj, Baldev., (2007). Effect of initial pH and temperature of iron salt solutions on formation of magnetite nanoparticles. Elsevier. Materials chemistry and Physics 103168-175.
- [11]. Zhang, B., Xing, J., Liu, H., 2007. Preparation and application of magnetic microsphere carriers. Higher Education Press and Springer-Verlag. Front. Chem. Eng. China, 1(1): 96-101. DOI 10.1007/s11705-007-0019-3.
- [12]. Günzler, H., Gremlich, H., 2002. IR Spectroscopy. Wiley-VCH Verlag GmbH. Alemania.
- [13]. Kim, K. 2007. Synthesis and characterization of magnetite nanopowders. Current Applied Physics. DOI: 10.1016/j.cap.2007.04.021.
- [14]. Lian, S., Wang, E., Kang, Z., Bai, Y., Gao, L., Jiang, M., Hu, C., Xu, L. 2004. Synthesis of magnetite nanorods and porous hematite nanorods. Elsevier Solid State Communications 129 485-490.
- [15]. Yang, P., Yu, J., Wu, T., Liu, G., Chang, T., Lee, D., Cho, D., 2004. Urea decomposition method to synthesize hidrotalcites. Chinese Chemical Letters. Vol. 15, No. 1, pp 90-92. <http://www.imm.ac.cn/journal/ccl.html>
- [16]. Xu, L., Hu, C., Jiang, M., Wang, E., Kang, Z., Lian, S. (2003). Convenient synthesis of single crystalline magnetic Fe₃O₄ nanorods. Solid State Communications 127 (2003) 605-608.
- [17]. Kobayashi, B., Saeki, S., Yoshida, M., Nagao, D., Konno, M., 2007. Synthesis of spherical submicron-sized magnetite/silica nanocomposite particles. Springer Science+Business Media, LLC. DOI 10.1007/s10971-007-1648-1.
- [18]. Liu, Xianquiao., Ma, Zhiya., Xing, Jianmin., Liu, Huizhou. 2004. Preparation and characterization of amino-silane modified superparamagnetic silica nanospheres. Journal of Magnetism and magnetic Materials 270 1-6.
- [19]. Xing, J., Zhang, B., Lang, Y., Liu, H. 2008. Synthesis of amino-silane modified magnetic silica adsorbents and application for adsorption of flavonoids from *Glycyrrhiza uralensis Fisch.*
- [20]. Yu, C., Tam, K., Lo, C., Tsang, S., 2007. Functionalized silica coated magnetic nanoparticles with biological species for magnetic separation. IEEE Transactions on magnetics, Vol. 43, No. 6. DOI 10.1109/TMAG.2007.894203.
- [21]. Yamaura, M., Camilo, R., Sampaio, L., Macedo, M., Nakamura, M., Toma, H., 2004. Preparation and characterization of (3-aminopropyl) triethoxysilane-coated magnetite nanoparticles. Journal of Magnetism and Magnetic Materials 279 (2004) 210-217.
- [22]. Ma, M., Zhang, Y., Yu, W., Shen, H., Zhang, H., Gu, N., 2002. Preparation and characterization of magnetite nanoparticles coated by aminosilane. Colloids and Surfaces A: Physicochem Eng. Aspects: 212 (2003) 219-226. Elsevier Science B.V. PH: S0927-7757(02)00305-9.
- [23]. Y. Ivanova, Ts. Gerganova, H. M. H. V. Fernandes*, I. M. Miranda, E. Kashchieva Journal of the University of Chemical Metallurgy, Vol.41, No.3, 311-316 (2006).